AIAA JOURNAL
Vol. 45, No. 9, September 2007

Spectrally Accurate Prediction of Sonic Boom Signals

Anthony R. Pilon*
Lockheed Martin Aeronautics Company, Palmdale, California 93599

DOI: 10.2514/1.28159

The development of a new sonic boom prediction methodology is discussed. By solving Burgers' equation, the new method is able to predict accurately the thickness of the shock waves in a boom signal, resulting in a smoothly varying, continuous signal. The resultant signal allows for spectral analysis and the calculation of sonic boom noise metrics. The effects of aircraft maneuvers and accelerations, as well as signal propagation through a real, stratified, windy atmosphere are taken into account through a ray tracing approach. The new method is efficient and accurate, making it a useful tool in the development of supersonic cruise aircraft.

Nomenclature

A_r	=	oxygen relaxation dissipation and dispersion coefficient
a	=	speed of sound
B_r	=	nitrogen relaxation dissipation and dispersion coefficient
C_{tv}	=	thermoviscous dissipation coefficient
f	=	frequency
k	=	wave number
L	=	atmospheric length scale
$\hat{P}$	=	Fourier transform of the pressure signal
p'	=	acoustic pressure
s	=	propagation distance
t	=	time
t'	=	retarded time
$\hat{\alpha}$	=	atmospheric absorption coefficient
Γ	=	Gol'dberg number
γ	=	ratio of specific heats
Δx_d	=	dissipation propagation distance
Δx_s	=	shock formation distance
λ	=	wavelength
ρ	=	density
ω	=	cyclic frequency

Subscripts

$\circ$	=	ambient air quantities

I. Introduction

SONIC boom signals are produced by the nonlinear propagation of shock waves and pressure disturbances generated by supersonically traveling aircraft, missiles, artillery projectiles, and so on [1]. The startle and annoyance caused by these impulsive, high-amplitude sound signals have hampered previous attempts at the development of civil supersonic transport aircraft. For example, the Anglo–French Concorde was not allowed to fly supersonically over land because of the unacceptable public response to the high-amplitude sonic boom signals it generated.

In spite of the challenges presented by the sonic boom phenomenon, supersonic cruise flight remains a goal for many in the aerospace industry who have concluded that business jets with supersonic cruise capabilities are technically feasible. However, allowable supersonic flight over land may be required for a supersonic business jet to be profitable. Therefore, the sonic boom signals must be "minimized" to reduce or eliminate public annoyance. Sonic boom minimization theory was developed by Seebass, George, and others [2,3] in the 1960s, and was recently proved to be credible for the first time by the Defense Advanced Research Projects Agency/NASA sponsored Shaped Sonic Boom Demonstration (SSBD) and Shaped Sonic Boom Experiment (SSBE) programs [4,5]. The flight vehicle developed for these programs showed that it is possible to reduce the perceived loudness of an aircraft's sonic boom through deliberate and judicious contouring of the aircraft shape. Reductions in startle and annoyance can be expected corresponding to the reductions in perceived loudness.

Some means of quantifying the "loudness," "noisiness," or "intensity" of a sonic boom signal will be required to determine what signals, and therefore what type of supersonic cruise aircraft, will be acceptable for supersonic overland flight. Calculation of these noise metrics, for example, the perceived level (PL) metric of Stevens [6], or the C-weighted sound exposure level [7], will require accurate prediction of the spectral content of the sonic boom signals.

This paper outlines the development of a prediction methodology that is accurate enough to resolve the spectral characteristics of a sonic boom signal, while taking into account the effects of propagation through a real atmosphere, winds, aircraft maneuvers, and so on. Additionally, the code has the ability to account for the possibly complicated interactions and reflections that occur when a propagating sonic boom signal reaches the ground. Spectral analysis of predicted sonic boom signals and calculation of acceptability metrics are automated in the code.

Modern sonic boom prediction processes are discussed in the next section. The following section contains a discussion of the nonlinear propagation algorithm employed in the new code. This is followed by an outline of the ray tracing algorithm employed in the new method. Next is a discussion of the calculation of noise metrics and ground interaction effects. Validation calculations and sample predictions are then presented, followed by concluding remarks and a discussion of possible future work.

II. Sonic Boom Prediction Process

There are three steps that must be taken in the prediction of sonic boom signals generated by supersonic aircraft. The first step is to determine the static pressure signal in the aircraft near-field. Often, this near-field signal is extracted from a computational fluid dynamics (CFD) solution of the flow around the aircraft. If the aircraft is accelerating or maneuvering, the signal must be generated or suitably modified to take the time dependent nature of the maneuvers into account. The near-field signal must be generated close enough to the aircraft that the numerical dissipation inherent in

Presented as Paper 2449 at the 12th AIAA/CEAS Aeroacoustics Conference (27th AIAA Aeroacoustics Conference), Cambridge, MA, 8–10 May 2006; received 3 October 2006; revision received 7 May 2007; accepted for publication 7 May 2007. Copyright © 2007 by Lockheed Martin Corporation. Published by the American Institute of Aeronautics and Astronautics, Inc., with permission. Copies of this paper may be made for personal or internal use, on condition that the copier pay the $10.00 per-copy fee to the Copyright Clearance Center, Inc., 222 Rosewood Drive, Danvers, MA 01923; include the code 0001-1452/07 $10.00 in correspondence with the CCC.

*Senior Staff Engineer, Advanced Development Programs, 1011 Lockheed Way. Associate Fellow AIAA.

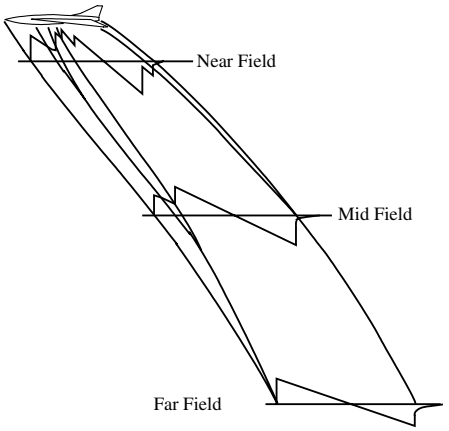

Fig. 1 Sonic boom generation and propagation: wave-front viewpoint.

CFD solvers does not destroy the fidelity of the signal. However, the signal must also be determined far enough away from the aircraft to not have cross flow and lift distribution effects dominate the propagation in the next step. The second step in boom prediction is to nonlinearly propagate the pressure signal to the receiver location on or near the ground. If the boom signal is propagated through a nonuniform or windy atmosphere, ray tracing and geometric acoustics are employed to determine the propagation path and the effects of acoustical spreading. The third step in sonic boom prediction is to calculate the effects of the boom signal's interaction with the ground, and calculate applicable noise metrics for assessment. The sonic boom prediction code in development is designed to accomplish the second and third steps listed above. The production of near-field pressure signals in the first step is dependent on CFD solvers or wind tunnel measurements, and is not a part of the current development effort. Figure 1 shows a schematic of the generation and propagation of a sonic boom from the aircraft or wave-front viewpoint.

III. Nonlinear Propagation

Sonic boom signals are the result of nonlinear propagation of high-amplitude static pressure disturbances, that is, sound, away from supersonic cruise vehicles. In this section, the nonlinear propagation theory employed in the new method is outlined.

The nonlinear propagation of sound in the atmosphere is governed by Burgers' equation. The solution of Burgers' equation for nonlinear plane wave propagation employed in the current method follows that outlined by Cleveland [8]. The lossless form of Burgers' equation is

$$\frac{\partial p'}{\partial x} = \frac{\beta}{2\rho_\circ a_\circ^3}\frac{\partial (p')^2}{\partial t'} \tag{1}$$

where p' is the acoustic (disturbance) pressure, x is the propagation distance, $\rho_\circ$ is the ambient air density, $a_\circ$ is the ambient air speed of sound, t' is the retarded time, and β is the coefficient of nonlinearity. For sound propagation in air, $\beta = (\gamma + 1)/2$, where γ is the ratio of specific heats. If the pressure signal at any point along the propagation path is taken as

$$p'(x, t') = f(t) \tag{2}$$

then the solution at $x + \Delta x$ is

$$p'(x + \Delta x, t') = f\left(t' + \frac{p'\beta \Delta x}{\rho_\circ a_\circ^3}\right) \tag{3}$$

The second term on the right side above determines the nonlinear distortion of the signal, and can lead to multivalued waveforms. Before a waveform becomes multivalued, however, a shock (infinite slope in the pressure signal) is formed. The distance Δx_s from the current point on the propagation path, at which a shock first forms, can be determined by calculating the location where the slope of the pressure signal becomes infinite, so that

$$\Delta x_s = \frac{\rho_\circ a_\circ^3}{\beta \cdot \max(\frac{\partial f}{\partial t'})} \tag{4}$$

In plane wave acoustic propagation, the signal is propagated along a line while calculating the local shock formation distance Δx_s. If the shock formation distance is less than the local marching step, the code propagates the shorter distance, and forms a zero-thickness shock in the solution. The pressure jumps and speed of the shocks formed in the signal are governed by the Rankine–Hugoniot relations [9]. The rest of the signal, away from the shocks, remains governed by the lossless Burgers' equation.

Figure 2 shows the nonlinear plane wave propagation of an initially sinusoidal signal. The signal becomes multivalued when the propagation distance $s > \Delta x_s$. (Here Δx_s is the shock formation distance of the initial sinusoidal waveform.) The dashed lines in parts d–f indicate where shock waves would form.

The theory presented above can be shown to be equivalent to the waveform parameter method of Thomas [10], if the effects of geometrical spreading are removed. However, the shock waves predicted have no thickness. The shock waves in sonic boom signals are affected by molecular relaxation and thermoviscous mechanisms in the atmosphere, which give them finite thickness, or "rise time." These effects are highly dependent on frequency, as well as ambient atmospheric properties (pressure, temperature, humidity, and so on). In the current method, the time domain signal determined through the lossless Burgers' equation algorithm described above is periodically (e.g., every 50 ft along the propagation path) resampled and Fourier transformed into the frequency domain with a fast Fourier transform (FFT) algorithm [11]. (This resampling causes the shocks to now have a small nonzero thickness.) With the signal in the frequency domain, frequency dependent coefficients for the attenuation of sound can be calculated

$$\hat{P}(\omega) = \hat{P}(\omega) e^{-\hat{\alpha}\Delta x_d} \tag{5}$$

where Δx_d is the distance propagated since the last application of dissipation, and $\hat{\alpha}$ is the complex atmospheric absorption coefficient. Following Cleveland [8] and Gee [12], the real and imaginary parts of $\hat{\alpha}$ can be expressed as

$$\Re[\hat{\alpha}(f)] = C_{\text{tv}} + A_r\left(\frac{f^2 f_{r,O}}{f^2 + f_{r,O}^2}\right) + B_r\left(\frac{f^2 f_{r,N}}{f^2 + f_{r,N}^2}\right) \tag{6}$$

$$\Im[\hat{\alpha}(f)] = A_r\left(\frac{f^3}{f^2 + f_{r,O}^2}\right) + B_r\left(\frac{f^3}{f^2 + f_{r,N}^2}\right) \tag{7}$$

where C_{tv} is a thermoviscous dissipation coefficient, A_r and B_r are relaxation coefficients for oxygen and nitrogen, and $f_{r,\text{O}}$ and $f_{r,\text{N}}$ are the relaxation frequencies of oxygen and nitrogen. These empirical quantities are dependent on the ambient temperature, temperature, and absolute humidity. They can be determined though the methods outlined in the applicable International Organization for Standardization (ISO) standard [13]. Figure 3 shows the variation of the real part of the complex atmospheric absorption coefficient with frequency for three altitudes and relative humidity levels in an ISO standard atmosphere. Similarly, Fig. 4 shows the variation of the imaginary part of the atmospheric absorption coefficient with frequency. The complex atmospheric absorption coefficient is recalculated whenever dissipative effects are applied in the current code.

After application of the dissipative and dispersive mechanisms, the inverse FFT algorithm is used to return the signal to the time domain. With the signal back in the time domain, the code continues the propagation, forming zero-thickness shocks as necessary. As the boom signal gets closer to the ground, attenuation increases,

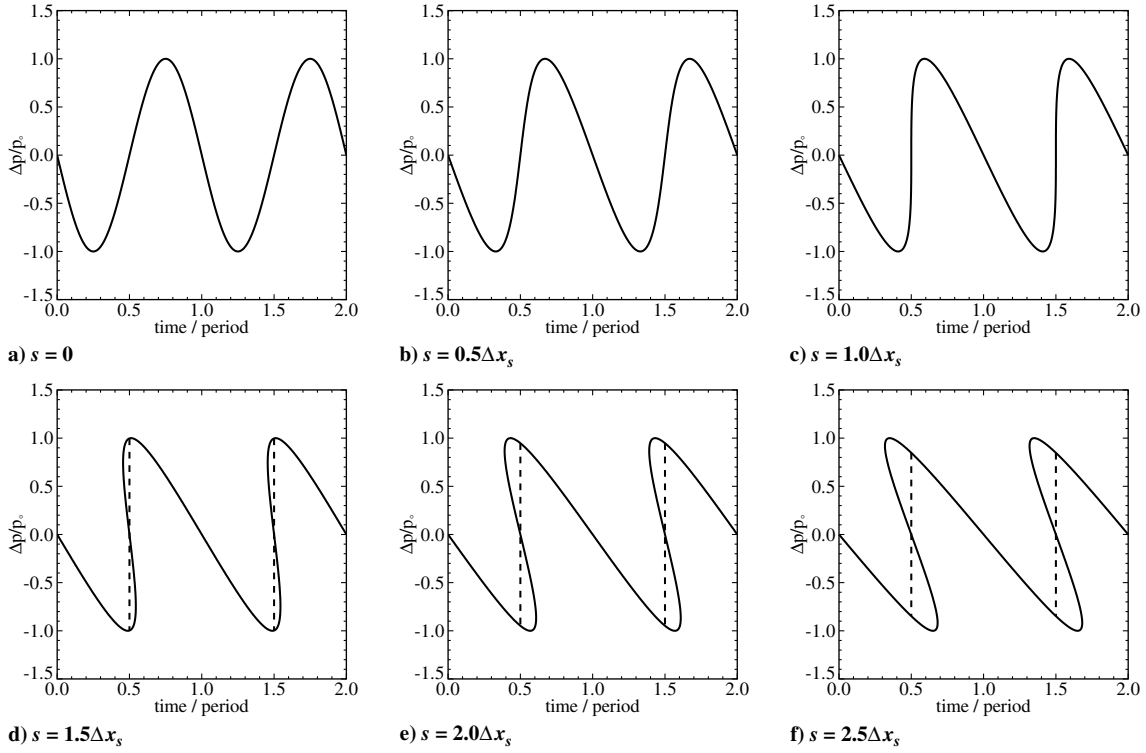

Fig. 2 Nonlinear acoustic propagation and shock formation. To prevent multivalued waveforms, shock waves are formed at the dashed lines. (Δx_s is the shock formation distance of the initial waveform.)

especially at high frequencies, and zero-thickness shocks no longer form, so that the final signal is smooth and continuous. The mixed time-frequency algorithm used in the nonlinear propagation portion of the method in development is similar in nature to the codes developed by Pestorius [14], Anderson [15], Bass and Raspet [16], and Robinson [17]. Cleveland et al. [18] present a comparison of several related Burgers' equation solvers for sonic boom propagation through uniform and isothermal atmospheres.

The current method differs from these codes in two ways. The first difference is in the prediction of a boom signal's interaction with the ground, which will be discussed below. The second difference lies in how the current tool handles the very thin, strong shock waves that form in boom signals at high altitudes, near the source aircraft. As discussed above, these strong shocks are modeled with zero-thickness steps in the current method. This approximation is also made in Robinson's code [17]. However, the current method resamples these step shocks so that they are one time step wide, and then applies the effects of atmospheric absorption as if the shocks were fully resolved. That is, the frequency-domain absorption algorithm does not distinguish between step shocks and the rest of the signal. This methodology automates the development and propagation of fully resolved shock waves from step shocks, but it can also introduce Gibbs oscillations in the time domain signals. The current method reduces these oscillations by forming two separate signals from the noisy signal. The first is generated using only the even-numbered points, the second with odd-numbered points. The two signals are then averaged to remove most of the Gibbs oscillations. Any remaining high-frequency noise is damped out by atmospheric absorption during propagation to the ground.

The process of forming and propagating step shocks as discussed above has an advantage that may not be readily apparent. Unlike the idealized signals used in the comparison study of Cleveland et al. [18], the near-field boom signals generated by actual flight vehicles often contain multiple compressions from negative to positive

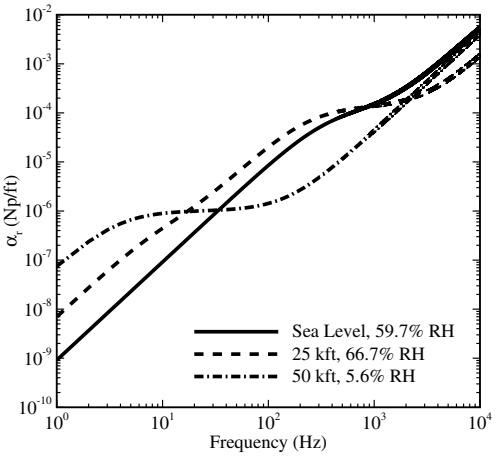

Fig. 3 Atmospheric dissipation coefficients.

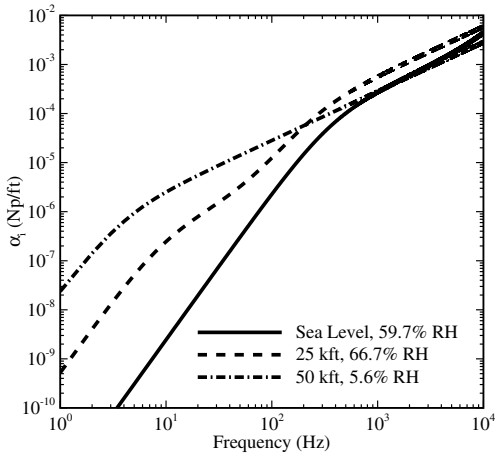

Fig. 4 Atmospheric dispersion coefficients.

acoustic pressure ("zero crossings"). If these compressions are strong enough, they will form shock waves during propagation. These shocks will move, relative to the rest of the signal, and they may merge with other shocks. If an attempt is made to resolve fully the shocks in a prediction tool based on the time domain solution of the lossless Burgers' equation, those shocks will not move relative to the rest of the signal. At a zero crossing, the solution to the lossless Burgers' equation becomes

$$p'(x + \Delta x, t') = f\left(t' + \frac{p'\beta\Delta x}{\rho_\circ a_\circ^3}\right) = f(t') = 0 \tag{8}$$

Thus, a zero crossing will always remain at the same retarded time, if step shocks are not formed and translated according to the Rankine–Hugoniot relations [9].

A. Fay Solution

A closed form solution for plane wave nonlinear propagation of initially sinusoidal signals was developed by Fay [19,20]. If the absorption coefficient is assumed to be constant, then Fay's solution is

$$p'(t) = \frac{2\alpha\rho_\circ a_\circ^3}{\omega\beta}\sum_{n=1}^{\infty}\frac{\sin[n(\omega t - kx)]}{\sinh[n\alpha(s + \Delta x_s)]} \tag{9}$$

This solution is valid for $s/\Delta x_s > 3$ and $\Gamma \geq 50$, where Γ is the Gol'dberg number, $\Gamma = 1/\alpha\Delta x_s$ [21]. Figure 5 compares the Fay solution with predictions obtained with the current method at 10 shock formation distances from the initial signal shown in Fig. 2, with $\Gamma = 60$. The excellent agreement validates the nonlinear propagation and dissipation processes in the current method.

B. Comparison with Low-Amplitude Sonic Boom Measurements

A series of sounding rocket flights were conducted near the NASA Dryden Flight Research Center. These flights were not related to sonic boom research, but the descent of the rockets from high altitude produced low-amplitude sonic boom signals on the ground. NASA engineers were able to record some of these signals [22]. Following the analysis of Plotkin et al. [22], the current method was used to propagate an initial zero-thickness step shock waveform for 100 s in a uniform atmosphere with a temperature of 68°F and a relative humidity of 30%. Plane wave propagation was assumed, due to the high altitude of the rocket generating the sonic boom. The shock predicted with this process is compared with the lead shock of the measured signal in Fig. 6. The qualitative agreement between the predicted and measured shock structures is excellent.

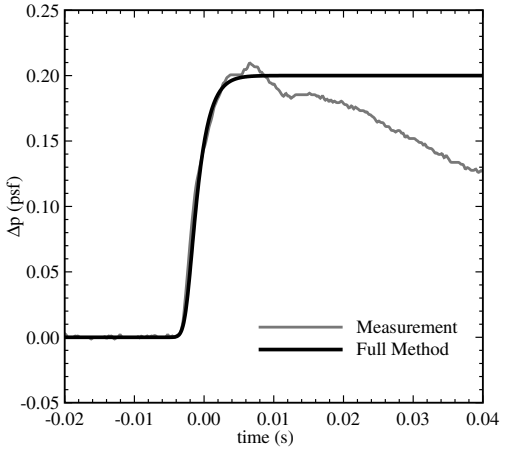

Fig. 6 Lead shock structure of predicted and measured low-amplitude sonic boom signals.

IV. Ray Tracing

The effects of sonic boom propagation through a stratified, moving atmosphere are predicted in the current method with a ray tracing and geometrical acoustics approach. Sound propagation in a layered atmosphere is considered, with ambient temperature, pressure, and sound speed varying with height above the Earth.

For sonic boom propagation through the atmosphere, it is usually valid to assume that the wavelength of the propagating sound is much less than the length scale of atmospheric gradients. Blokhintzev [23] presents the ray tracing equations for sound propagation through a layered atmosphere in the presence of winds. The ray tracing scheme employed in the current method is based on that presented by Thomas [10,24]. A predictor–corrector scheme is employed, marching in propagation time from the aircraft near-field location, through the layered atmosphere, to the listener at the ground. Each ray's initial trajectory is determined by the speed and direction of the aircraft. (For steady level flight, the initial trajectory is orthogonal to the aircraft Mach cone.) A ray tube, composed of four rays calculated with this marching approach, is used to determine the amplitude of the sonic boom signal. The four rays in each ray tube are separated in the near field by small increments in emission time and azimuth. Blokhintzev [23] shows that the signal amplitude is inversely proportional to the ray tube cross-sectional area at any time during propagation. If the aircraft is maneuvering or accelerating, a series of

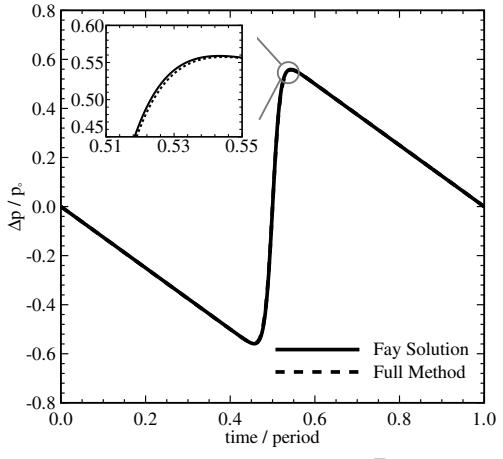

Fig. 5 Fay solution at $s = 10\Delta x$. $\Gamma = 60$.

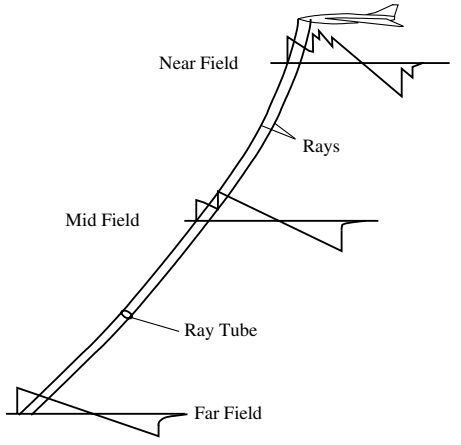

Fig. 7 Sonic boom generation and propagation: ray viewpoint.

ray tubes are calculated to capture the effects of the maneuver. The effects of nonlinearity in sonic boom signal propagation are calculated with the same approach used for nonlinear plane wave propagation. Sonic boom signal propagation from the ray viewpoint is depicted in Fig. 7.

Acceleration, maneuvering, or atmospheric winds will often cause the area of a ray tube to approach zero. Because the signal amplitude is inversely proportional to the ray tube area, considerable amplification of the sonic boom signals can occur. The current method is able to predict the amplification caused by finite ray tube areas. However, it cannot currently predict the sonic boom behavior at a caustic, where the ray tube cross-sectional area goes to zero. Future versions of the code in development will integrate a full nonlinear Tricomi equation solver [25,26] to predict the boom amplification effects near a caustic.

V. Ground Effects and Noise Metrics

When a sonic boom signal reaches a listener at the ground, reflections and absorptions can significantly alter the signal. Most current sonic boom prediction codes assume perfect reflections from hard ground planes, which leads to a doubling of the signal amplitude. A more complex ground reflection and attenuation model is included in the current method. This model accounts for soft or hard surfaces, variable incidence, and surface wave generation [27–29]. Experimentally recorded sonic boom data for soft ground surfaces and/or elevated microphones are not readily available, so this portion of the code has not been validated.

Prediction of the spectral content of a sonic boom signal is inherent in the calculation of atmospheric absorption in the current prediction methodology. As a result, the new method is ideally suited for the calculation of noise metrics. These metrics are useful for assessment of the perception, startle, and annoyance of sonic boom signals. The most promising of these metrics is the perceived level of Stevens [6], which has been shown to correlate well with human startle and annoyance [30]. When the current method finishes calculating a ground sonic boom signal, it automatically calculates the narrow band and one-third octave band power spectra. These spectra are then used to calculate the signal's perceived level, and the A-weighted, C-weighted, and flat-weighted sound exposure levels [7]. Thus, it will be useful for sonic boom assessment during the design phase of an aircraft development program.

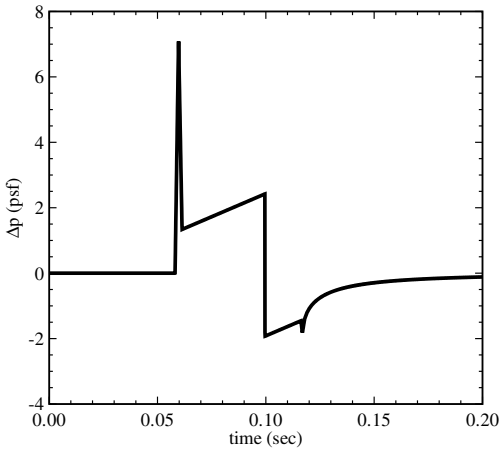

Fig. 8 Near-field minimized sonic boom signal.

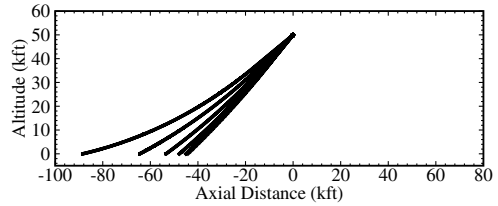

Fig. 9 Atmospheric propagation ray paths. The flight direction is right to left.

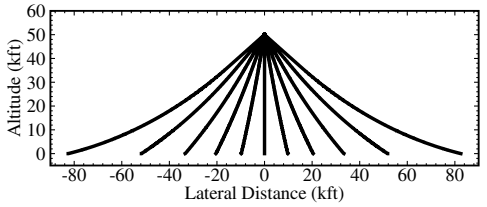

Fig. 10 Atmospheric propagation ray paths. The flight direction is out of the paper.

VI. Results and Discussion

The code in development has been compared with other sonic boom prediction codes and with experimental data. Results of two of those comparisons are presented here.

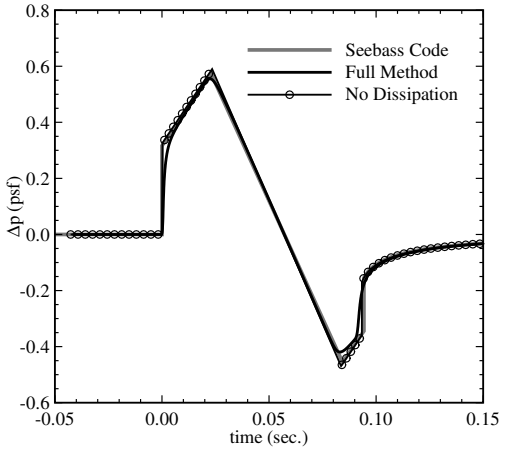

Fig. 11 Ground minimized sonic boom signals.

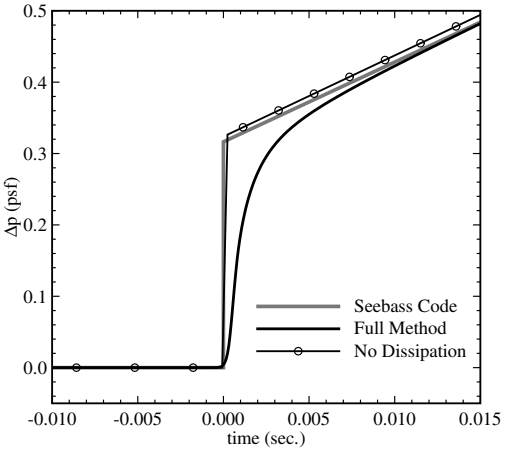

Fig. 12 Close-up view of the bow shocks in the ground sonic boom signals.

A. Comparison with Linear Minimization Theory

Darden [31] has developed a code to determine the equivalent area distributions, *F* functions, and resultant ground sonic boom signals for the minimization theory of Seebass et al. [2,3,32] The near-field signal (taken from the *F* function produced by this code) for a boom-minimized vehicle cruising at Mach 1.6 and 50,000 ft is shown in Fig. 8. The current method was used to propagate this signal to the ground through the ISO standard atmosphere [13]. Paths for rays that intersect the ground are shown in Figs. 9 and 10. The ground sonic boom signals, calculated with and without dissipative processes included, are compared with the theoretical minimized boom signal in Fig. 11. The three signals compare well, with minor differences caused by the nature of the atmospheric propagation and ground reflection algorithms in the codes. Figure 12 shows a close-up view of the lead shocks in the ground sonic boom signals. The smooth continuous signal predicted by the current method is apparent. Most of the audible energy in a sonic boom signal is contained in the shock waves. Therefore, determination of the shock-wave thickness is necessary for proper assessment of the signals.

B. Comparison with Flight Test Data

In January 2004, the SSBE program conducted a series of flight tests during which several near-field, in-flight, static pressure signals were measured below the SSBD aircraft. High-quality microphone recordings were also made at ground level, and on a glider below the SSBD flight path. The current method was used to propagate one of these near-field signals to ground level, through an atmosphere representative of the test-day conditions. The near-field signal chosen was signal number 2, from SSBE flight 31. When measuring this signal, the probe aircraft was approximately 74 ft (1.5 body lengths) below the SSBE aircraft, and lateral displacement was less than two degrees. The measured near-field signal is shown in Fig. 13. During the near-field measurements, the SSBE aircraft was flying at approximately 31,800 ft and Mach 1.38.

The near-field signal shown in Fig. 13 was propagated through an atmosphere representative of those experienced during testing. The

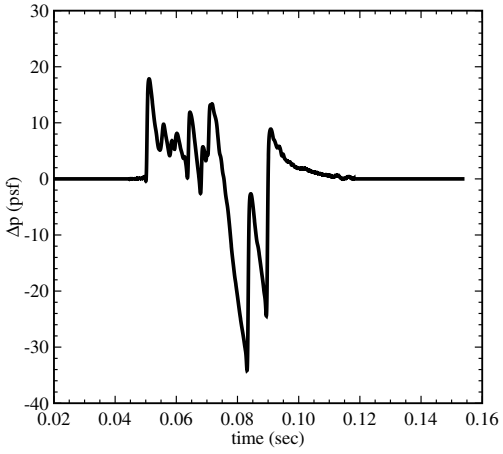

Fig. 13 Pressure signal approximately 74 ft below the SSBE vehicle.

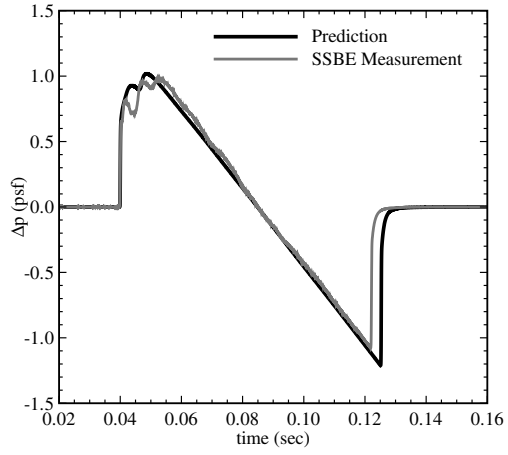

Fig. 14 Predicted and measured SSBE ground sonic boom signals.

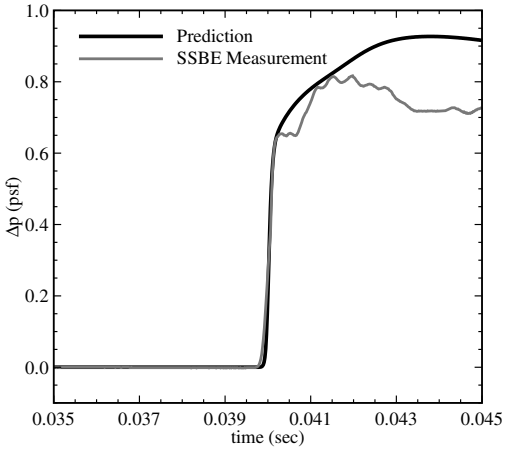

Fig. 15 Close-up view of the bow shocks in the predicted and measured SSBE ground sonic boom signals.

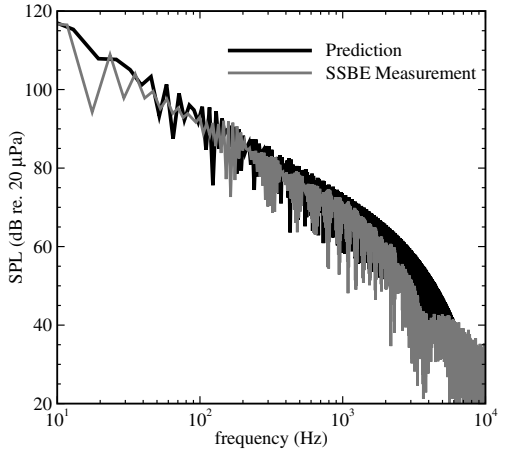

Fig. 16 Predicted and measured SSBE ground sonic boom power spectra.

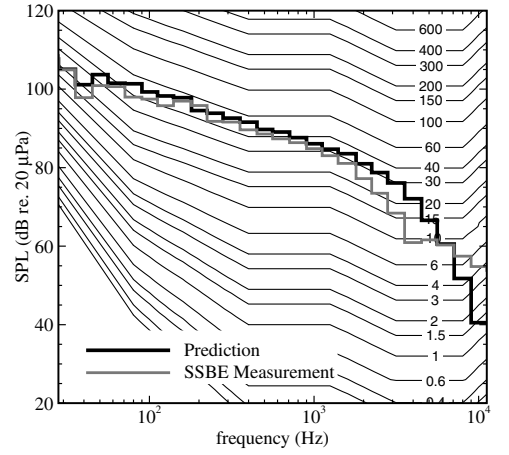

Fig. 17 Predicted and measured SSBE ground sonic boom third octave spectra. Stevens' contours of equal perceived magnitude, in sones, are shown for reference.

atmospheric pressure, temperature, wind speed, and direction recorded by a weather balloon during testing were used in the ray tracing and atmospheric absorption calculations. Figure 14 shows a comparison of the predicted ground boom signal with a ground microphone signal recorded during SSBE flight 21. (The predicted signal is compared with microphone data from a previous flight because flight 31 microphone data are corrupted by the presence of the probing aircraft in the SSBE near field.) The time domain signals compare remarkably well. A close-up view of the lead shock waves in the predicted and measured signals is shown in Fig. 15. Note that the effects of atmospheric turbulence were minimized in the recorded signal through the method outlined by Plotkin et al. [33,34]. In developing this method, they noted that the turbulent distortions behind both shocks in a recorded SSBE signal were roughly the same. And so, the noise from the aft shock to the end of the signal can be subtracted from the region following each shock, producing an approximate "turbulence-free" signal. Currently, the new method has no means of accounting for the effects of atmospheric turbulence, but those effects will need to be included in the assessment of the acceptability of any proposed supersonic cruise aircraft.

Predicted and measured sonic boom narrow band power spectra are shown in Fig. 16. The comparison is again good, with atmospheric effects and noise evident in the recorded signal. These spectra were used to determine the predicted and recorded signals' one-third octave band spectra, which are shown in Fig. 17. These spectra are plotted over the contours of equal perceived magnitude used in the calculation of Stevens' perceived level [6]. The perceived level of the measured signal, with the effects of turbulence minimized, is 105.0 PLdB, whereas the prediction yields 106.3 PLdB. The thinner shock waves of the predicted signal cause the slightly higher perceived level.

VII. Conclusions

A new sonic boom prediction methodology has been developed. The new method solves Burgers' equation with established numerical techniques [8,17,18], giving it the ability to predict accurately the thickness of the shock waves in a sonic boom signal. Thus, the predicted signals are smoothly varying and continuous. This allows for spectral analysis and the calculation of sonic boom noise metrics, without the need to add empirically derived thicknesses to the shock waves. The effects of boom signal propagation through stratified atmospheres and aircraft maneuvers are predicted with a geometric acoustics approach. The new method runs quickly on desktop computers, producing full sonic boom carpets in minutes. It automatically calculates noise metrics, making it a useful tool in the development of supersonic cruise aircraft.

Future work on the new method will involve the validation of the ground reflection and attenuation model, and the addition of capability to handle ray tube focusing, and the associated amplification of boom signals. The effects of atmospheric turbulence on sonic boom generation and propagation will be investigated and integrated with the new method.

Acknowledgments

The author would like to thank Ed Haering of NASA Dryden Flight Research Center, Ken Plotkin of Wyle Laboratories, and the Shaped Sonic Boom Experiment team for the data used in this effort.

References

[1] Plotkin, K. J., and Maglieri, D. J., "Sonic Boom Research: History and Future," AIAA Paper 2003-3575, 2003.

[2] Seebass, A. R., and George, A. R., "Design and Operation of Aircraft to Minimize Their Sonic Boom," *Journal of Aircraft*, Vol. 11, No. 9, 1974, pp. 509–517.

[3] Jones, L. B., "Lower Bounds for Sonic Bangs," *Journal of the Royal Aeronautical Society*, Vol. 65, No. 606, 1961, pp. 1–4.

[4] Plotkin, K. J., Page, J. A., Graham, D. H., Pawlowski, J. W., Schein, D. B., Coen, P. G., McCurdy, D. A., Haering, E. A., Murray, J. E., Ehernberger, L., Maglieri, D. J., Bobbitt, P. J., Pilon, A. R., and Salamone, J., "Ground Measurements of a Shaped Sonic Boom," AIAA Paper 2004-2923, 2004.

[5] Pawlowski, J. W., Graham, D. H., Boccadoro, C., Coen, P. G., and Maglieri, D. J., "Origins and Overview of the Shaped Sonic Boom Demonstration Program," AIAA Paper 2005-0005, 2005.

[6] Stevens, S. S., "Perceived Level of Noise by Mark VII and Decibels (E)," *Journal of the Acoustical Society of America*, Vol. 51, No. 2, 1972, pp. 575–601.

[7] Anon., "American National Standard Methods for Measurement of Impulse Noise," ANSI Standard S12.7-1986, 1986.

[8] Cleveland, R. O., "Propagation of Sonic Booms Through a Real, Stratified Atmosphere," Ph.D. Thesis, Univ. of Texas at Austin, Austin, TX, 1995.

[9] Pierce, A. D., *Acoustics: An Introduction to Its Physical Principles and Applications*, The Acoustical Society of America, Woodbury, NY, 1994, pp. 574–576.

[10] Thomas, C. L., "Extrapolation of Sonic Boom Pressure Signatures by the Waveform Parameter Method," NASA TN D-6832, June 1972.

[11] Press, W. H., Teukolsky, S. A., Flannery, B. P., and Vetterling, W. T., *Numerical Recipes in FORTRAN: The Art of Scientific Computing*, Cambridge Univ. Press, New York, 1992, pp. 490–515.

[12] Gee, K. L., "Prediction of Nonlinear Jet Noise Propagation," Ph.D. Thesis, Pennsylvania State Univ., University Park, PA, 2005.

[13] Anon., "Acoustics: Attenuation of Sound During Propagation Outdoors," ISO Standard 9613, 1993.

[14] Pestorius, F. M., "Propagation of Plane Acoustic Noise of Finite Amplitude," Ph.D. Thesis, Univ. of Texas at Austin, Austin, TX, 1973.

[15] Anderson, M. O., "Propagation of a Spherical *N*-Wave in an Absorbing Medium and its Diffraction by a Circular Aperture," Univ. of Texas at Austin, Tech. Rept. ARL-TR-74-25, Austin, TX, 1974.

[16] Bass, H. E., and Raspet, R., "Propagation of Medium Strength Shock Waves Through the Atmosphere," *Journal of the Acoustical Society of America*, Vol. 64, No. 4, 1978, pp. 1208–1210.

[17] Robinson, L. D., "Sonic Boom Propagation Through an Inhomogeneous Windy Atmosphere," Ph.D. Thesis, Univ. of Texas at Austin, Austin, TX, 1991.

[18] Cleveland, R. O., Chambers, J. P., Bass, H. E., Raspet, R., Blackstock, D. T., and Hamilton, M. F., "Comparison of Computer Codes for the Propagation of Sonic Boom Waveforms Through Isothermal Atmospheres," *Journal of the Acoustical Society of America*, Vol. 100, No. 5, 1996, pp. 3017–3027.

[19] Fay, R. D., "Plane Sound Waves of Finite Amplitude," *Journal of the Acoustical Society of America*, Vol. 3, Oct. 1931, pp. 222–241.

[20] Beyer, R. T., *Nonlinear Acoustics*, Acoustical Soc. of America, Woodbury, NY, 1997, p. 112.

[21] Gol'dberg, Z. A., "On the Propagation of Plane Waves of Finite Amplitude," *Soviet Physics—Acoustics*, Vol. 3, 1957, pp. 340–347.

[22] Plotkin, K. J., Haering, E. A., and Murray, J. E., "Low-Amplitude Sonic Boom from a Descending Sounding Rocket," *Innovations in Nonlinear Acoustics*, edited by A. A. Atchley, V. W. Sparrow, and R. M. Keolian, American Inst. of Physics, Melville, NY, 2005.

[23] Blokhintzev, D. I., "Propagation of Sound in an Inhomogeneous and Moving Medium I," *Journal of the Acoustical Society of America*, Vol. 18, No. 2, 1946, pp. 322–328.

[24] Thomas, C. L., "Extrapolation of Wind-Tunnel Sonic Boom Signatures Without Use of a Whitham *F*-Function," NASA SP-255, Oct. 1970, pp. 205–217.

[25] Auger, T., and Coulouvrat, F., "Numerical Simulation of Sonic Boom Focusing," *AIAA Journal*, Vol. 40, No. 9, 2002, pp. 1726–1734.

[26] Marchiano, R., Coulouvrat, F., and Grenon, R., "Numerical Simulation of Shock Wave Focusing at Fold Caustics, with Application to Sonic Boom," *Journal of the Acoustical Society of America*, Vol. 114, No. 4, 2003, pp. 1758–1771.

[27] Chien, C. F., and Soroka, W. W., "Sound Propagation Along an Impedance Plane," *Journal of Sound and Vibration*, Vol. 43, No. 1, 1975, pp. 9–20.

[28] Chien, C. F., and Soroka, W. W., "A Note on the Calculation of Sound Propagation Along an Impedance Surface," *Journal of Sound and Vibration*, Vol. 69, No. 2, 1980, pp. 340–343.

[29] Delany, M. E., and Bazley, E. N., "Acoustical Properties of Fibrous Absorbent Materials," *Applied Acoustics*, Vol. 3, No. 2, 1970, pp. 105–116.

[30] Leatherwood, J. D., Sullivan, B. M., Shepherd, K. P., McCurdy, D. A., and Brown, S. A., "Summary of Recent NASA Studies of Human Response to Sonic Booms," *Journal of the Acoustical Society of America*, Vol. 111, No. 1, 2002, pp. 599–619.

[31] Darden, C. M., "Sonic Boom Minimization with Nose Bluntness

Relaxation," NASA TP 1348, 1979.
[32] Carlson, H. W., "The Lower Bound of Attainable Sonic-Boom Overpressure and Design Methods of Approaching This Limit," NASA TN D-1494, Oct. 1962.
[33] Plotkin, K. J., Maglieri, D. J., and Sullivan, B. M., "Measured Effects of Turbulence on the Waveforms and Loudness of Sonic Booms," *Innovations in Nonlinear Acoustics*, edited by A. A. Atchley, V. W. Sparrow, and R. M. Keolian, American Inst. of Physics, Melville, NY, 2005.
[34] Plotkin, K. J., Maglieri, D. J., and Sullivan, B. M., "Measured Effects of Turbulence on the Loudness and Waveforms of Conventional and Shaped Minimized Sonic Booms," AIAA Paper 2005-2949, 2005.

X. Zhong
Associate Editor